Detailed magnetization study of quenched random ferromagnets. I. Low-lying magnetic excitations

S. N. Kaul* and P. D. Babu
School of Physics, University of Hyderabad, Central University P.O., Hyderabad-500 134, Andhra Pradesh, India
(Received 23 December 1993)

Magnetization as a function of temperature has been measured for amorphous (a-) $(Fe_pNi_{1-p})_{80}B_{19}Si_1$ ($0.0625 \le p \le 0.2$), $(Fe_pNi_{1-p})_{80}B_{20}$ ($0.25 \le p \le 1.0$), and $(Fe_pNi_{1-p})_{80}P_{14}B_6$ ($0.1125 \le p \le 1.0$) alloys in the temperature range 3.8–300 K at various constant applied magnetic-field values in the interval $5 \le H \le 15$ kOe. An elaborate data analysis reveals the following. (i) For all p in the a-$(Fe_pNi_{1-p})_{80}(B,Si)_{20}$ alloy series, the contribution to the thermal demagnetization due to single-particle (SP) excitations of the *weak* itinerant type, though present at all temperatures, is completely dominated by that arising from spin-wave (SW) excitations in the temperature range $0 \lesssim t\ (=T/T_C) \lesssim t^*(p)$ but the reverse is true for $t > t^*(p)$. However, in a-$(Fe_pNi_{1-p})_{80}P_{14}B_6$ alloys, SP excitations of the weak itinerant type give a feeble contribution, which is masked by the SW contribution, for temperatures up to $0.9T_C$ (300 K) in the concentration range $0.1125 \le p \le 0.25$ ($0.375 \le p \le 0.625$) but for $T \lesssim 300$ K and $p \gtrsim 0.75$, a *significant* SP contribution of the *strong* itinerant type accompanies a dominant SW contribution. (ii) The spin-wave stiffness coefficient D in both the alloy series, as in fcc Fe_xNi_{100-x} alloys, varies with temperature as $D(T) \sim T^{5/2}$ and $D(T) \sim T^2$ for Fe concentrations below and above $x = 80p = 60$ at. %, respectively. (iii) The direct exchange interactions extend beyond the second nearest-neighbor distance for compositions close to, but above, the critical concentration for the appearance of long-range ferromagnetic order whereas the competing interactions in the alloy with $p > 0.75$ confine the direct exchange to the nearest neighbors only. The observation (i) above is shown to imply that all the compositions in the a-$(Fe_pNi_{1-p})_{80}$ $(B,Si)_{20}$ alloy series behave as *weak* itinerant ferromagnets while a transition from *weak* itinerant to *strong* itinerant ferromagnetism occurs at $p \simeq 0.75$ in the a-$(Fe_pNi_{1-p})_{80}P_{14}B_6$ alloy series. Arguments are presented to show that the property D_n (inelastic neutron scattering) $\gg D_m$ (magnetization) of the alloys with $p > 0.75$ in both the alloy series studied is a consequence of the fact that the longitudinal spin fluctuations make as significant a contribution to the $T^{3/2}$ decrease of magnetization as the transverse spin fluctuations (spin waves) do, but leave D_n unaltered from its "spin-wave-only" value.

I. INTRODUCTION

Extensive experimental investigations have been carried out during the past two decades on a large number of amorphous ferromagnetic alloys with a view to unraveling the nature of low-lying magnetic excitations in them. Inelastic neutron scattering (INS) experiments[1–14] have demonstrated that such noncrystalline materials do exhibit well-defined long-wavelength (magnon wave vector $q \to 0$) spin-wave (SW) excitations (up to temperatures as high as $0.8T_c$) which follow a normal ferromagnetic dispersion relation[15]

$$E_q(T) = \hbar\omega_q(T) = \Delta + D(T)q^2(1-\beta q^2)\ , \tag{1}$$

where $\Delta(\sim 0.05$ meV) is an effective energy gap originating primarily from the dipole-dipole interactions, $\langle r^2 \rangle = 20\beta$ is the second moment of the exchange interaction given by

$$\langle r^2 \rangle = \frac{\int r^2 J(r) G(r) dr}{\int J(r) G(r) dr} \tag{2}$$

[in Eq. (2), $J(r)$ is the exchange integral and $G(r)$ is the radial distribution function of the magnetic atoms], and the SW stiffness coefficient D renormalizes with temperature according to the relation

$$D(T) = D(0)(1 - D_{5/2}T^{5/2}) \tag{3}$$

predicted by the Heisenberg model which takes into account the magnon-magnon interactions. Such measurements are, however, limited to low transferred momenta (typically $q \le 0.2$ Å^{-1}) and hence to small scattering angles due to the lack of periodicity in amorphous ferromagnets. At higher momentum transfer values, the spin waves appear to be diffused. Consistent with the above dispersion relation [Eq. (1)], thermal demagnetization of spontaneous magnetization $M(T)$ and average magnetic hyperfine field $\overline{H}_{\rm hf}(T)$ at low temperatures is adequately described by the expression[4–6,8,10,14,16–34]

$$\begin{aligned}\Delta M(T)/M(0) &= [1 - \{M(T)/M(0)\}] \\ &= [1 - \{\overline{H}_{\rm hf}(T)/\overline{H}_{\rm hf}(0)\}] \\ &= BT^{3/2} + CT^{5/2} + \cdots\ ,\end{aligned} \tag{4}$$

where the coefficients B and C of the $T^{3/2}$ and $T^{5/2}$ terms are related to the coefficients of q^2 and q^4 terms in Eq. (1) as

$$B = \xi(3/2)[g\mu_B/M(0)](k_B/4\pi D)^{3/2} \tag{5}$$

and

$$C = 15\pi\beta\xi(5/2)[g\mu_B/M(0)](k_B/4\pi D)^{5/2} . \quad (6)$$

In Eqs. (5) and (6), $\xi(3/2)=2.612$ and $\xi(5/2)=1.341$ are the Riemann zeta functions. However, the values D_m of the SW stiffness coefficient deduced from the magnetization and Mössbauer measurements with the aid of Eqs. (4)–(6), though in remarkably good agreement with one another, are lower by a factor ~ 2 than those D_n directly determined from INS experiments in a large number of glassy ferromagnets that exhibit Invar behavior.[6,12,35] Alternatively, $D_m \simeq D_n$ for non-Invar ferromagnetic systems only.[4,9,12,26,30,31] Several arguments[1–3,12,36–40] put forward to justify such a discrepancy between D_m and D_n are summarized below. (a) As already mentioned above, a complete absence of translational invariance in amorphous ferromagnets restricts the INS measurements to q values[1,2] $\lesssim 0.2$ Å^{-1} whereas the coefficient B of the $T^{3/2}$ term in Eq. (4) is the "thermal average" of the total contribution arising from spin waves of all wave lengths. (b) Besides the conventional spin waves, there exist additional excitations, invisible to neutrons, which also decreases magnetization according to the Bloch $T^{3/2}$ law and are more or less localized in nature. (c) Continentino and Rivier[36] contend that in amorphous ferromagnets with a noncollinear ground-state arrangement of local magnetic moments (caused by a strong competition between ferromagnetic and antiferromagnetic interactions), the diffusive modes ("diffusions") originating from the longitudinal spin fluctuations contribute to the $T^{3/2}$ decrease of magnetization as significantly as the transverse spin fluctuations (spin waves) do. But, unlike conventional spin waves, the diffusions show up as a broad central peak in the constant-q INS intensity versus energy scans. (d) Ishikawa *et al.*[6] attribute the rapid thermal demagnetization in Invar alloys to an anomalous spin-wave damping mechanism in that the SW linewidths in them follow the empirical relation

$$\Gamma_q(T) \propto \Gamma_0(1+cT^a)q^2 , \quad (7)$$

where $a \approx 1$, instead of the variation with q and temperature of the type

$$\Gamma_q(T) \propto [T \ln(k_B T/E_q)]^2 q^4 \quad (8)$$

predicted by the Heisenberg model that accounts for the magnon-magnon interactions. (e) In amorphous ferromagnets, the spin-wave peaks have a finite linewidth due to random fluctuation in the magnitude of local spins or in the strength of exchange interactions between neighboring spins or in both. The SW linewidth increases rapidly as the magnon wavelength decreases and, as a consequence, the coefficient of the $T^{3/2}$ term in Eq. (4) is substantially enhanced[37] compared to the value predicted by conventional spin-wave theory, which strictly holds for extremely narrow SW linewidths. (f) Considering that the itinerant character of magnetic electrons manifests itself in both[30,38,39] the Invar behavior and the large single-particle contribution, besides the SW contribution, to $\Delta M(T)/M(0)$, Kaul[40] argues that a total neglect of the single-particle contribution while analyzing the $\Delta M(T)/M(0)$ data for Invar alloys is basically responsible for the wide disparity between D_m and D_n in such systems.

With the exception of (d) and (f), all the above-mentioned arguments fail to explain why D_n equals D_m for some amorphous (a-) ferromagnetic alloys. Contrary to the claim made by Ishikawa *et al.*,[6] recent high-resolution INS data[11,12,14] on a number of amorphous Invar alloys, which also include the compositions in the a-$Fe_{100-x}B_x$ alloy series previously studied by Ishikawa *et al.*,[6] reveal that the SW linewidths in such systems vary with q and T in accordance with Eq. (8). From the validity of Eq. (8) and a relatively large magnitude of the coefficient $D_{5/2}$ in Eq. (3) for amorphous Invar alloys, Fernandez-Baca and co-workers[11,12,14] concluded that a rapid decline of magnetization with temperature in these Invar systems is due to additional excitations (diffusions), as proposed by Continentino and Rivier,[36] and not from anomalous spin-wave linewidths.[6,37] But, as already stated above, it is not clear why diffusions should be present in the amorphous Invar systems only. Conflicting results have also been reported with regard to the argument (f). Yamada and co-workers[32,33] concluded that a-$Fe_{100-x}B_x$ ($12 \le x \le 21$) Invar alloys are weak itinerant ferromagnets and the Stoner single-particle contribution to $\Delta M(T)/M(0)$ varies as T^2 whereas Babic, Marohnic, and Wohlfarth[41] contend that a-$Fe_{80}B_{20}$ and a-$Fe_xNi_{80-x}B_{18}Si_2$ ($15 \le x \le 60$) alloys are strong itinerant ferromagnets and the Stoner contribution to $\Delta M(T)/M(0)$ varies as $T^{3/2}\exp(-\Delta/k_BT)$. Even though the results of both these investigations are consistent with each other in that the additional single-particle contribution is necessary to reproduce the observed thermal demagnetization in these systems, Hasegawa and Ray[22] assert that spin-wave excitations alone do completely account for $\Delta M(T)/M(0)$ in a-$Fe_{100-x}B_x$ ($12 \le x \le 28$) alloys. Furthermore, in direct contradiction with the conclusions drawn by Babic, Marohnic, and Wohlfarth,[41] spontaneous resistivity anisotropy,[42,43] high-field susceptibility,[43] spin-polarized photoemission,[44] and Compton scattering[45] studies on numerous amorphous Fe-Ni-based $3d$ transition-metal–metalloid glasses reveal that the alloys with Fe concentration ranging between 10 and 82 at. % are weak itinerant ferromagnets.

From the foregoing text, it is evident that a complete knowledge about the nature of low-lying magnetic excitations in amorphous ferromagnets is still lacking. With a view to gaining more physical insight into this aspect of amorphous magnetism, high-precision magnetization measurements on amorphous $(Fe_pNi_{1-p})_{80}(B,Si)_{20}$ and $(Fe_pNi_{1-p})_{80}P_{14}B_6$ alloys were undertaken.

II. EXPERIMENTAL DETAILS

Amorphous (a-) $(Fe_pNi_{1-p})_{80}P_{14}B_6$ ($0.038 \le p \le 1.0$), $(Fe_pNi_{1-p})_{80}B_{19}Si$ ($0.025 \le p \le 0.2$), and $(Fe_pNi_{1-p})_{80}B_{20}$ ($0.25 \le p \le 1.0$) alloys were prepared in the ribbon form (typical cross section 2×0.03 mm^2) under high-purity argon atmosphere by the single-roller melt-quenching technique. Note that the alloys with $p < 0.25$ in the a-

$(Fe_pNi_{1-p})_{80}B_{20}$ alloy series cannot be obtained in the amorphous state unless 1 at. % boron is replaced by silicon. The amorphous nature of the ribbons so fabricated was first verified by the x-ray diffraction method using Mo $K\alpha$ radiation and then confirmed by the high-resolution electron microscopic (HREM) technique. The ribbons that did not reveal any crystalline regions upon HREM examination were used for the present magnetization studies. A detailed compositional analysis[46] of the alloys in question, using a JEOL FCS four-crystal (wavelength-dispersive) spectrometer in conjunction with a JSM 35 JEOL scanning electron microscope as well as the inductive coupled plasma technique, revealed that the actual Fe (Ni) concentration p did not differ from the nominal value by more than $\pm 0.002(\pm 0.002)$ in any case. Magnetization (M) of the as-quenched alloy ribbons was measured as a function of temperature (T) to a relative accuracy of 10 ppm in the temperature range 3.8–300 K at several fixed values of the applied magnetic field (H) in the interval $5 \leq H \leq 15$ kOe during the cooling cycle (typical cooling rate 0.5 K min^{-1}) by the Faraday method. The M versus H isotherm was recorded for each composition at 1.6 K in fields up to 20 kOe using a PAR vibrating-sample magnetometer after cooling the sample in a field of 1 kOe (the field at which thermomagnetic irreversibility, associated with the reentrant behavior at low temperatures, is completely suppressed). From such an isotherm, the spontaneous magnetization at 0 K is obtained as an intercept on the ordinate when the linear high-field portion of the M vs H curve is extrapolated to $H=0$. In all the measurements, H was applied along the length within the ribbon plane in order to minimize the demagnetizing effects. The sample temperature was monitored by precalibrated carbon-glass and platinum-resistance sensors in the temperature ranges 3.8–50 K and 50–300 K, respectively.

III. RESULTS AND DATA ANALYSIS

The magnetic phase diagrams in the entire composition range covered in the present experiments are shown in Fig. 1 for amorphous $(Fe_pNi_{1-p})_{80}(B,Si)_{20}$ (series I) and

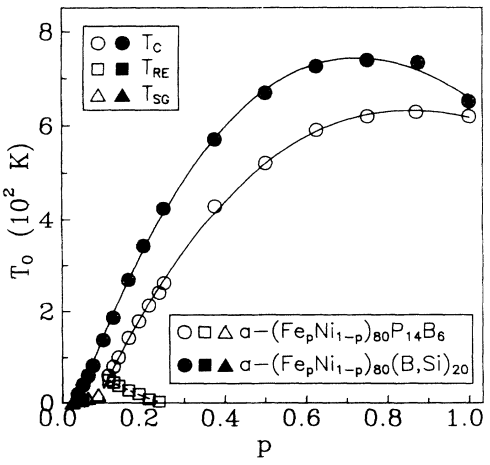

FIG. 1. Magnetic phase diagrams for amorphous $(Fe_pNi_{1-p})_{80}(B,Si)_{20}$ and $(Fe_pNi_{1-p})_{90}P_{14}B_6$ alloys.

$(Fe_pNi_{1-p})_{80}P_{14}B_6$ (series II) alloys. In these diagrams, T_C and T_{SG} denote the temperatures at which the transition from the paramagnetic (PM) to ferromagnetic (FM) and from PM to spin-glass (SG) states take place while T_{RE} ($\ll T_C$) represents the temperature at which a strong irreversibility in the low-field ($\lesssim 100$ Oe) magnetization occurs. Alternatively, $T_{RE}(H)$ marks the temperature at which field-cooled and zero-field-cooled magnetizations corresponding to a given field strength H (in the low-field region) bifurcate and $T_{RE}=\lim_{H\to 0}T_{RE}(H)$. T_C, T_{RE}, and T_{SG} have been accurately determined[26,30,46–50] from ac (zero-field) susceptibility, electrical resistivity, and bulk magnetization measurements performed on different compositions in the above-mentioned glassy alloy series. It is noticed from Fig. 1 that at $p=\bar{p}_c$ ($\simeq 0.03$ and 0.10 for the series I and II, respectively) all the four phases, namely, PM, FM, RE (reentrant), and SG, coexist with one another. Since the main concern of this paper is to study low-lying magnetic excitations in the FM phase of the alloy series in question, all the relevant magnetic parameters, including T_C, are listed in Tables I and II but no details about the nature of the RE and SG phases and the transitions at T_{RE} and T_{SG} are furnished here.

According to the theories[15] based on the localized-electron model, the thermal demagnetization of spontaneous magnetization $M(0,T)$ is solely due to spin-wave excitations and hence $M(0,T)/M(0,0)\sim T^{3/2}(\sim T^{3/2}+T^{5/2})$ at low (intermediate) temperatures. By contrast, the theoretical calculations[51,52] based on the itinerant-electron model predict that $M(0,T)$ should decrease with increasing temperature as $[M(0,T)/M(0,0)]_{SW}\sim T^{3/2}$ at low temperatures, $[M(0,T)/M(0,0)]^2_{LSF}\sim T^2$ ($[M(0,T)/M(0,0)]_{SP}\sim T^2$) over a wide range of intermediate temperatures, and $[M(0,T)/M(0,0)]^2_{LSF}\sim T^{4/3}$ for temperatures close to T_C if, besides spin-wave excitations, both Stoner single-particle (SP) excitations and local spin-density fluctuations (LSF) (only SP excitations) contribute to $M(0,T)$. With a view to arriving at the exact functional dependence of the in-field magnetization $M(H,T)$ on temperature, the reduced magnetization $M(H,T)/M(H,0)$ is plotted against T^2 and $T^{3/2}$ for a-$Fe_{80}B_{20}$ in Fig. 2(a) whereas the reduced magnetization squared, $[M(H,T)/M(H,0)]^2$, is plotted against T^2 and $T^{4/3}$ for the same alloy in Fig. 2(b). The main features of the data presented in Fig. 2 are characteristic of other compositions in both the alloy series. It is evident from this figure that the in-field magnetization follows closely the functional form $[M(H,T)/M(H,0)]\simeq 1-BT^{3/2}$ for $T\lesssim 140$ K and $[M(H,T)/M(H,0)]=1-AT^2$ for temperatures in the range $140\lesssim T\lesssim 300$ K; the other functional forms [Fig. 2(b)] do not fit the $M(H,T)$ data in any temperature range below 300 K. The above finding asserts that (i) local spin-density fluctuations, if present, are completely suppressed[53] by external magnetic fields as high as 9 kOe and (ii) the observed temperature dependence of the relative deviation of magnetization from its value at 0 K (no distinction between the values of $M(H,T)$ at 3.8 and 0 K is made in this work), i.e., $[M(H,0)-M(H,T)]/M(H,0)\equiv\Delta m(T)$, should be ana-

TABLE I. Splitting factor g, density ρ, spin-wave and other relevant magnetic parameters, and mean-square range of the exchange interaction $\langle r^2 \rangle$ for a-$(Fe_pNi_{1-p})_{80}(B,Si)_{20}$ alloys. Numbers in parentheses denote the estimated uncertainty in the least significant figure while those within the square brackets are the values of $\langle r^2 \rangle$ expressed in terms of the average nearest-neighbor distance $\bar{a} \simeq 2.55$ Å.

p	g	ρ (g/cm^3)	$M(0,0)$ (emu/g)	T_C (K)	$D(0)$ (meV Å^2)	$D_{5/2}$ (10^{-7} K$^{-5/2}$)	D_2 (10^{-6} K^{-2})	A (10^{-6} K^{-2})	$D(0)/T_C$ (meV Å^2/K)	$\langle r^2 \rangle$ (Å^2) [$\bar{a}^2$] Eq. (17)	$\langle r^2 \rangle$ (Å^2) [$\bar{a}^2$] Eq. (18)
0.0375		8.11		19.00(5)							
0.0500		8.10		40.00(5)							
0.0625	2.06(2)	8.09	25.78(12)	60.00(5)	35.7(3)	1.17(30)			0.595(5)	0.6(2) [0.09]	27.6(2) [4.24]
0.0750	2.06(2)	8.08	29.71(13)	82.50(5)	41.2(3)	1.25(25)			0.500(5)	1.0(2) [0.15]	23.2(2) [3.57]
0.1000	2.06(2)	8.06	36.64(15)	137.50(5)	50.6(3)	1.15(30)			0.368(5)	2.0(5) [0.31]	17.1(2) [2.63]
0.1250	2.07(2)	8.04	42.93(10)	186.50(5)	58.5(5)	1.20(30)			0.314(5)	3.5(10) [0.54]	14.6(2) [2.25]
0.1625	2.07(2)	8.01	51.82(8)	268.50(5)	69.0(5)	1.20(20)			0.257(3)	6.3(12) [0.97]	11.9(1) [1.83]
0.2000	2.07(2)	7.98	60.71(9)	342.00(10)	76.0(5)	1.20(30)		3.60(1)	0.222(3)	9.4(26) [1.45]	10.3(1) [1.58]
0.2500	2.06(2)	7.94	71.80(5)	425.00(10)	89.0(5)	0.80(20)		3.20(1)	0.209(2)	11.0(30) [1.69]	9.7(1) [1.49]
0.3750	2.07(2)	7.83	98.15(5)	571.00(10)	111.0(5)	0.46(2)		1.50(5)	0.193(2)	14.4(10) [2.21]	9.0(1) [1.38]
0.5000	2.08(2)	7.49	122.00(5)	669.00(20)	128.0(10)	0.50(2)		1.02(2)	0.191(2)	27.0(20) [4.15]	8.9(1) [1.37]
0.6250	2.08(2)	7.38	142.41(5)	725.00(30)	144.0(10)	0.58(20)		0.81(3)	0.199(2)	48.3(185) [7.43]	9.2(1) [1.41]
0.7500	2.07(2)	7.28	159.29(5)	738.00(40)	146.0(10)		1.50(20)	0.78(6)	0.197(2)		9.2(1) [1.41]
0.8750	2.09(2)	7.17	176.36(5)	733.00(50)	124.0(15)		1.30(20)	0.82(4)	0.169(2)		7.9(1) [1.21]
1.0000	2.10(2)	7.08	185.09(5)	651.00(30)	92.0(20) 170.0(250)[a]		1.35(10)	1.21(1)	0.141(3)		6.6(1) [1.01]

[a]Value of $D(0)$ determined by Brillouin scattering (Ref. 5).

TABLE II. Splitting factor g, density ρ, spin-wave and other relevant magnetic parameters, and mean-square range of the exchange interaction $\langle r^2 \rangle$ for a-$(Fe_pNi_{1-p})_{80}P_{14}B_6$ alloys. Numbers in parentheses denote the estimated uncertainty in the least significant figure while those within the square brackets are the values of $\langle r^2 \rangle$ expressed in terms of the average nearest-neighbor distance $\bar{a} \simeq 2.55$ Å.

p	g	ρ (g/cm^3)	$M(0,0)$ (emu/g)	T_C (K)	$D(0)$ (meV Å^2)	$D_{5/2}$ (10^{-7} K$^{-5/2}$)	D_2 (10^{-6} K^{-2})	A' (10^{-6} K^{-2})	Δ/k_B (K)	$D(0)/T_C$ (meVÅ^2/K)	$\langle r^2 \rangle$ (Å^2) [$\bar{a}^2$] Eq. (17)	$\langle r^2 \rangle$ (Å^2) [$\bar{a}^2$] Eq. (18)
0.1125	2.09(2)	7.84	26.70(10)	56.00(5)	31.0(5)	1.20(10)				0.554(10)	0.4(1) [0.06]	25.7(5) [3.95]
0.1250	2.08(2)	7.83	30.60(10)	77.00(5)	34.5(5)	1.15(10)				0.448(7)	0.6(1) [0.09]	20.8(3) [3.20]
0.1375	2.07(2)	7.82	33.90(10)	94.00(5)	38.5(5)	1.22(10)				0.410(5)	1.0(1) [0.15]	19.0(2) [2.92]
0.1625	2.09(2)	7.80	40.00(5)	136.00(5)	45.0(5)	1.20(8)				0.331(4)	1.6(2) [0.25]	15.4(2) [2.37]
0.1875	2.06(2)	7.78	45.45(5)	171.00(5)	51.0(5)	1.25(8)				0.298(3)	2.6(2) [0.40]	13.8(1) [2.12]
0.2125	2.07(2)	7.76	50.90(5)	210.00(5)	57.0(5)	1.00(10)				0.271(2)	3.1(4) [0.48]	12.6(1) [1.94]
0.2375	2.09(2)	7.74	55.84(6)	252.00(5)	61.5(5)	0.85(8)				0.244(2)	3.5(4) [0.54]	11.3(1) [1.74]
0.2500	2.09(2)	7.73	58.36(4)	271.00(10)	64.0(5)	0.80(10)				0.236(2)	3.8(5) [0.58]	11.0(1) [1.69]
0.3750	2.11(2)	7.63	81.35(5)	430.00(10)	84.0(10)	0.50(10)				0.195(3)	6.3(15) [0.97]	9.1(1) [1.40]
0.5000	2.12(2)	7.52	104.67(5)	520.00(10)	99.0(10) 112.0(10)[a]	0.37(5) 0.60(5)[a]				0.190(2)	8.9(15) [1.37]	8.8(1) [1.35]
0.6250	2.12(2)	7.43	124.87(5)	590.00(20)	104.0(10)	0.45(8)				0.176(2)	14.4(30) [2.21]	8.2(1) [1.26]
0.7500	2.10(2)	7.33	139.67(5)	619.00(30)	105.0(10)		1.00(6)	1.2(2)	116(12)	0.170(2)		7.9(1) [1.21]
0.8750	2.11(2)	7.23	153.89(5)	628.00(50)	106.0(10)		1.20(5)	1.2(2)	157(35)	0.169(2)		7.9(1) [1.21]
1.0000	2.12(2)	7.14	166.50(5)	617.00(50)	100.0(20)		1.30(5)	1.2(2)	151(30)	0.162(3)		7.5(1) [1.15]

[a]Value of $D(0)$ and $D_{5/2}$ evaluated from the Fig. 5 of Ref. 9.

lyzed[54] in terms of the expression

$$\Delta m(T)=\Delta m_{SW}(T)+\Delta m_{SP}(T)\ , \tag{9}$$

where the spin-wave Δm_{SW} and Stoner single-particle Δm_{SP} contributions to Δm are given by[15,51]

$$\Delta m_{SW}(T)=\frac{g\mu_B}{M(H,0)}\left[Z(3/2,t_H)\left[\frac{k_BT}{4\pi D(T)}\right]^{3/2}+15\pi\beta Z(5/2,t_H)\times\left[\frac{k_BT}{4\pi D(T)}\right]^{5/2}\right] \tag{10}$$

and

$$\Delta m_{SP}(T)=\begin{cases}A'(H)T^{3/2}\exp(-\Delta/k_BT) & \text{for a strong itinerant ferromagnet ,} \quad (11a)\\ A(H)T^2 & \text{for a weak itinerant ferromagnet .} \quad (11b)\end{cases}$$

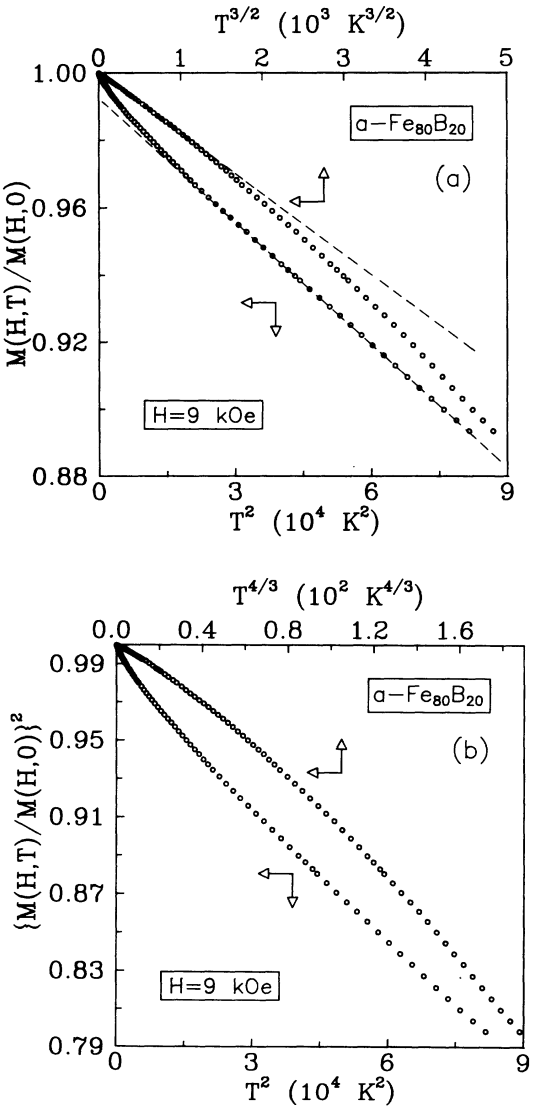

FIG. 2. (a) Reduced magnetization $M(H=9,\ \text{kOe},T)/M(H=9\ \text{kOe},0)$ versus T^2 and $T^{3/2}$ for a-$Fe_{80}B_{20}$. The dashed straight lines serve to highlight the temperature variation in a given temperature range. (b) Reduced magnetization squared, $[M(H=9,\ \text{kOe},\ T)/M(H=9\ \text{kOe},\ 0)]^2$, versus T^2 and $T^{4/3}$ for a-$Fe_{80}B_{20}$.

In Eq. (10), the Bose-Einstein integral functions

$$Z(s,t_H)=\xi(s)F(s,t_H)=\sum_{n=1}^{\infty}n^{-s}\exp(-nt_H) \tag{12a}$$

and

$$t_H=T_g/T=g\mu_BH_{\text{eff}}/k_BT \tag{12b}$$

allow for the extra energy gap $g\mu_BH_{\text{eff}}(=k_BT_g)$ in the spin-wave spectrum arising from the effective field

$$H_{\text{eff}}=H-4\pi NM+H_A \tag{13}$$

(where N,M and H_A are the demagnetizing factor, magnetization, and anisotropy field, respectively), which the spins experience within the sample. Alternatively, in the presence of the external magnetic field H, the magnon dispersion relation retains the form given by Eq. (1) but now Δ is replaced by $\Delta+g\mu_BH_{\text{eff}}$. For both localized-electron[15] and itinerant-electron[51,55] models, spin-wave stiffness $D(T)$ renormalizes with temperature according to the relation

$$D(T)=D(0)(1-D_2T^2-D_{5/2}T^{5/2})\ . \tag{14}$$

Within the framework of the Heisenberg model, the T^2 term appears in the expression for $D(T)$ if the localized d spins interact with one another via conduction s electrons whereas the $T^{5/2}$ term arises from the magnon-magnon interactions; the T^2 term is, however, several orders of magnitude smaller than the $T^{5/2}$ term since the s-d interaction is very weak compared to the direct d-d interaction. By contrast, the T^2 term in the itinerant-electron model results from the interaction between spin waves and single-particle excitations and dominates over the $T^{5/2}$ term, which originates from the magnon-magnon interactions, as in the localized-electron case. The expressions

$$D(T)=D(0)(1-D_2T^2) \tag{15}$$

and

$$D(T)=D(0)(1-D_{5/2}T^{5/2})\ , \tag{16}$$

are, therefore, used in this paper to denote the variation of the spin-wave stiffness coefficient with temperature

predicted by the itinerant- and localized-electron models, respectively.

Making use of the values of the demagnetizing factor N deduced from the low-field magnetization measurements and those of the splitting factor g as well as of the anisotropy field H_A reported in the literature,[30,56,57] theoretical fits to the $\Delta m(T)$ data have been attempted based on Eqs. (9)–(13) with $D(T)$ in Eq. (10) given by either Eq. (15) or Eq. (16). While attempting such fits with the aid of the least-squares (LS) method, all the possibilities have been covered, i.e., Eqs. (9), (10), and (11a) or (11b) involving the combinations $D(T)=D(0)$, $D(T)=D(0)(1-D_2T^2)$, and $D(T)=D(0)(1-D_{5/2}T^{5/2})$ with $\beta=A'$ (or A)$=0$ (i.e., higher-order spin-wave terms in Eq. (10) as well as the single-particle contribution $\Delta m_{\rm SP}(T)$ in one [Eq. (11a)] or the other [Eq. (11b)] form, are completely dropped) or $\beta=0$, A' (or A) $\neq 0$, or $\beta\neq 0$, A' (or A)$=0$ have been used for the fits to the $\Delta m(T)$ data. In order to ascertain the relative importance of the spin-wave and single-particle contributions to Δm within the temperature range covered in the present experiments, a range-of-fit analysis has been carried out in which the values of free fitting parameters in the above-mentioned theoretical fits are monitored as the temperature interval $T_{\rm min}\leq T\leq T_{\rm max}$ is progressively narrowed down by keeping $T_{\rm min}$ ($T_{\rm max}$) fixed and lowering (raising) $T_{\rm max}$($T_{\rm min}$) in 3 K steps towards $T_{\rm min}$($T_{\rm max}$). The successive (fixed) values of $T_{\rm min}$($T_{\rm max}$) differ by $t=T/T_C=0.1$ and include the lowest (highest) temperature for a given composition. Typical results of this type of analysis, when $T_{\rm max}$ is varied, are displayed in Fig. 3. Similar results are obtained when $T_{\rm min}$ is varied. In these plots, we define a reduced sum of deviation squares χ_r^2 as χ^2 for the $M(H,T)$ data in a given temperature interval divided by the total number of data points (N) in that interval minus the number of free fitting parameters ($N_{\rm para}$), i.e., $\chi_r^2=\chi^2/(N-N_{\rm para})$. The main reason for preferring χ_r^2 to χ^2 is that this choice permits an unambiguous assessment of the quality not only of a given type of fit as function of $T_{\rm max}$ or $T_{\rm min}$ but also of different types of fits in the same temperature interval. The following conclusions can be drawn from a close examination of the data presented in Fig. 3. (i) Temperature renormalization of spin-wave stiffness cannot be ignored, as is evident from the observation that all the fitting parameters exhibit wild variations and χ_r^2 diverges for $T_{\rm max}>130$ K for the least-squares fits based on the theoretical expressions that set $D(T)=D(0)$, whereas the fitting parameters are far more stable over a wide range of $T_{\rm max}$ values and χ_r^2 possesses considerably lower values for the LS fits based on the expressions that allow D to vary with T in accordance with Eq. (15) or (16). (ii) Irrespective of the type of fit attempted, χ_r^2 is consistently lower for the fits that employ Eq. (15) than those that use Eq. (16). Hence the functional dependence of D on T is better described by Eq. (15) than by Eq. (16). (iii) Regardless of the temperature range chosen for the fit, inclusion of the higher-order spin-wave term [the $T^{5/2}$ term in Eq. (10)] or the single-particle contribution [either of the weak itinerant type, Eq. (11b), or of the strong itinerant type, Eq. (11a)] besides the $T^{3/2}$ term in Eqs. (9) and (10) leaves values for the parameters of the $T^{3/2}$ fit [i.e., the LS fit that makes use of Eqs. (9) and (10) with $\Delta m_{\rm SP}(T)=\beta=0$] practically unaltered and does not bring forth any significant improvement in the quality of the fit (i.e., a marginal reduction in χ_r^2 occurs by the inclusion of these terms). Moreover, the coefficient of the additional term [i.e., the coefficient β of the $T^{5/2}$ term in Eq. (10) or the coefficient A of the T^2 term in Eq. (11b) or the coefficient A' of the $T^{3/2}\exp(-\Delta/k_BT)$ term in Eq. (11a)] invariably possesses a negligibly small value. The above observations (i)–(iii) obviously point to the fact that, out of the different types of fits whose results are depicted in Fig. 3, the one based on the theoretical expression that combines Eqs. (9), (10), and (15) and sets $\Delta m_{\rm SP}=\beta=0$ describes the observed temperature dependence of Δm the best. However, when the LS fit to the $\Delta m(T)$ data, based on Eq. (11b) alone, is attempted, χ_r^2 is reduced by an order of magnitude for $T>140$ K compared to the above-mentioned best fit but the reverse is true for $T<140$ K. This finding is consistent with the observations made earlier based on the data presented in Fig. 2. Another important point to note is that the best fits for all the compositions yield the values for $M(H,0)$ which agree with the experimentally measured values at 1.6 K to within 0.5%. Such an elaborate data analysis is called for because most earlier determinations[4–6,8,10,14,16–34] of the spin-wave stiffness coefficient for amorphous ferromagnets, including our own,[26,30,34] are seriously flawed in that they do not take into account the temperature renormalization of the spin-wave stiffness (even though INS data clearly demonstrate that appreciable reduction in spin-wave stiffness occurs with increasing temperature), or the single-particle contribution, or the effect of the external magnetic field.

Judging by the values of χ_r^2 and by the stability of the fitting parameters against a wide variation in $T_{\rm min}$ and $T_{\rm max}$, the main observations, based on the results of the range-of-fit analysis, can be summarized as follows. (i) For the alloys with $p\leq 0.625[p\geq 0.75]$ in series I, the theoretical expression which combines Eqs. (9) and (10) while setting $\Delta m_{\rm SP}(T)$ in Eq. (9) and β in Eq. (10) equal to zero and uses Eq. (16) [Eq. (15)] for $D(T)$ in Eq. (10) forms the best description of the observed variation of Δm with T for $t\leq t^*(p)$ whereas for all the alloys in series I Eq. (11b) alone [i.e., $\Delta m(T)=\Delta m_{\rm SP}(T)=A(H)T^2$] provides the best fit to the $\Delta m(T)$ data for $t>t^*(p)$. Contrasted with this behavior, Eq. (9) with $\Delta m_{\rm SP}(T)$ given by Eq. (11a) and $\Delta m_{\rm SW}(T)$ given by the version of Eq. (10) in which $\beta=0$ and $D(T)=D(0)(1-D_{5/2}T^{5/2})[=(D(0)(1-D_2T^2)]$ for $p\leq 0.625[p\geq 0.75]$ [this type of spin-wave contribution is henceforth referred to as $\Delta\bar{m}_{\rm SW}(T)$] closely reproduces the observed $\Delta m(T)$ for $t\lesssim 0.9$ for $p\leq 0.25$ and $T\leq 300$ K for $p\geq 0.375$ in the alloy series II. (ii) In alloy series I, single-particle excitations of the weak itinerant type [Eq. (11b)], though present at all temperatures, are completely overshadowed by the spin-wave contribution of the type $\Delta\bar{m}_{\rm SW}(T)$ for $t\leq t^*(p)$ but they completely account for the observed $\Delta m(T)$ for $t>t^*(p)$. By comparison,

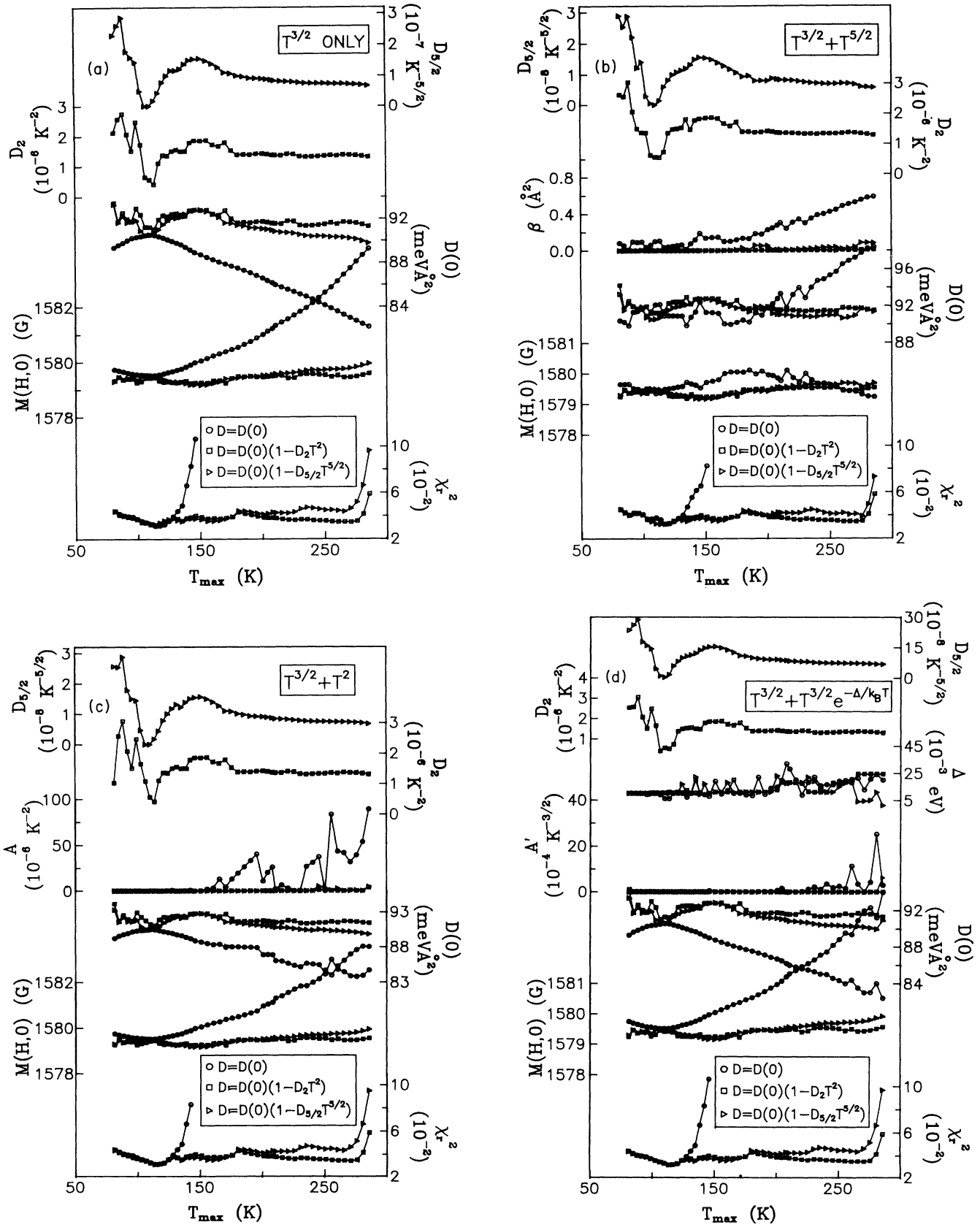

FIG. 3. Variation of the free fitting parameters with the upper limit (T_{max}) of the temperature range $T_{min} \leq T \leq T_{max}$ when T_{min} is kept fixed at 4.2 K and the least-squares fits to the $M(H=9$ kOe,$T)$ data are attempted based on (a) Eqs. (9) and (10) with $\beta=\Delta m_{SP}=0$, (b) Eqs. (9) and (10) with $\Delta m_{SP}=0$, (c) Eqs. (9), (10), and (11b) with $\beta=0$, and (d) Eqs. (9), (10), and (11a) with $\beta=0$, and, in each case, $D(T)$ in Eqs. (10) given by $D(T)=D(0)$ (open circles), or Eq. (15) (open squares), or Eq. (16) (open triangles).

single-particle excitations of the strong itinerant type [Eq. (11a)] significantly contribute, besides a dominant spin-wave contribution $\Delta\tilde{m}_{SW}(T)$, to $\Delta m(T)$ in the entire temperature range $T \leq 300$ K only for $p \geq 0.75$ in the alloy series II; for $p \leq 0.625$ in series II the spin-wave contribution $\Delta\tilde{m}_{SW}(T)$ to $\Delta m(T)$ is so large as to render an exact estimation of $\Delta m_{SP}(T)$ nearly impossible. The latter inference is drawn from the observation that, regardless of the temperature range chosen for the fit, inclusion of the single-particle contribution of the form given by Eq. (11b) or (11a) in addition to $\Delta\tilde{m}_{SW}(T)$ brings forth marginal or even no (marked) improvement in the quality of fits for $p \leq 0.625$ ($p \geq 0.75$) in series II as compared with the fits that consider only the $T^{3/2}$ term in Eq. (10) and set $\Delta m_{SP}=0$ in Eq. (9). (iii) The quality of the least-squares fits to $\Delta m(T)$ data based on the theoretical expressions that set $D(T)=D(0)$ is much worse compared with those that allow D to vary with T in accordance with either Eq. (15) or Eq. (16); the existing fits are also able to distinguish clearly between the cases where Eq. (15) or Eq. (16) is more appropriate to describe $D(T)$, e.g., the functional dependence of D on T is better described by Eq. (16) [Eq. (15)] than by Eq. (15) [Eq. (16)] for $p \leq 0.625$ [$p \geq 0.75$] in both the alloy series.

The continuous curves through the data points in Figs. 4 and 5 represent the best LS fits to the $\Delta m(T)$ data with the choice of the parameters given in Tables I and II. These tables list the values of other relevant physical quantities as well. The presently determined values of $M(0)$, $D(0)$, T_C, $D_{5/2}$, D_2, and A are displayed in Figs. 6 and 7 together with the values for these parameters in the case of fcc Fe_xNi_{100-x} crystalline (c-) alloys.[58,59] Note that in Figs. 6 and 7 the subscript p, which denotes the Fe composition in the alloy series I and II, has been changed to $x(=80p)$ in order to facilitate a direct comparison between the presently determined parameter values for the amorphous alloy series in question and those previously reported for crystalline Fe_xNi_{100-x} alloys. Figure 7 also depicts the variation of the so-called cross-over temperature t^* with x for a-$Fe_xNi_{80-x}(B,Si)_{20}$ alloys. In addition, the values of the mean-square range of the exchange interaction, $\langle r^2 \rangle$, are computed from the

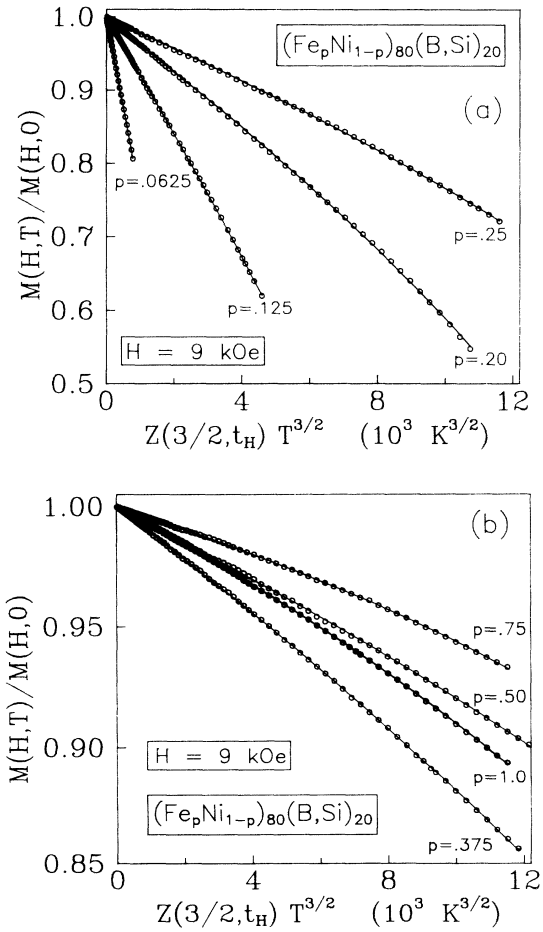

FIG. 4. Modified Bloch law behavior of the in-field magnetization for a few representative compositions in the amorphous $(Fe_pNi_{1-p})_{80}(B,Si)_{20}$ alloy series. The continuous curves through the data points represent the best least-squares fits (see text for details).

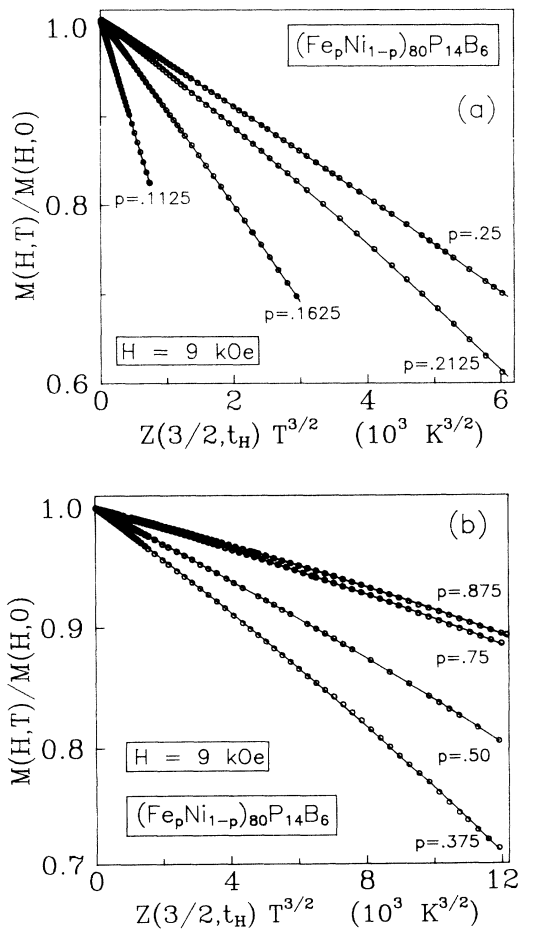

FIG. 5. Modified Bloch law behavior of the in-field magnetization for a few representative compositions in the amorphous $(Fe_pNi_{1-p})_{80}P_{14}B_6$ alloy series. The continuous curves through the data points represent the best least-squares fits (see text for details).

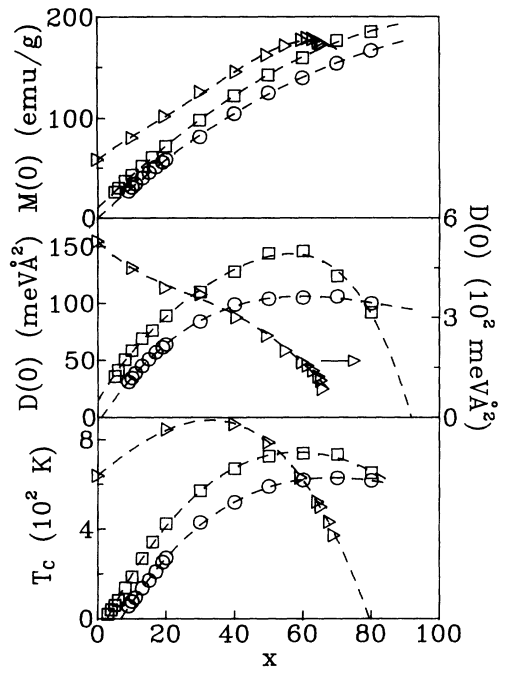

FIG. 6. Spontaneous magnetization at 0 K, $M(0)$, spin-wave stiffness coefficient at $T=0$ K, $D(0)$, and Curie temperature T_C as functions of the Fe concentration x in the amorphous $Fe_xNi_{80-x}(B,Si)_{20}$ (open squares) and $Fe_xNi_{80-x}P_{14}B_6$ (open circles) alloys and in fcc Fe_xNi_{100-x} crystalline alloys (open triangles, data taken from Refs. 58 and 59). The dashed curves through the data points serve as a guide to the eye.

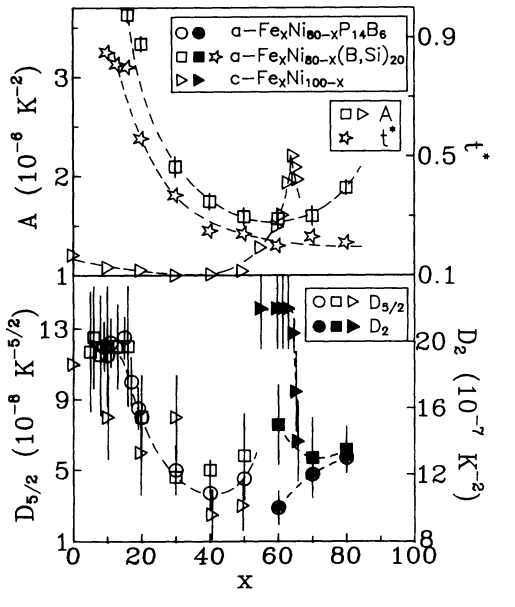

FIG. 7. Coefficients A, D_2, and $D_{5/2}$ [appearing in Eqs. (11b), (15), and (16) of the text] as well as the crossover temperature t^* as functions of the Fe concentration x in amorphous $Fe_xNi_{80-x}(B,Si)_{20}$ and $Fe_xNi_{80-x}P_{14}B_6$ alloys and in fcc Fe_xNi_{100-x} crystalline alloys (data taken Ref. 58).

relations[26,30,40]

$$D_{5/2}=\pi\xi(5/2)\left[\frac{g\mu_B}{M(0)}\right]\left[\frac{k_B}{4\pi D(0)}\right]^{5/2}\langle r^2\rangle \tag{17}$$

and

$$\frac{D(0)}{T_C}=\frac{(S/3)\int r^2J(r)G(r)dr}{[2S(S+1)/3k_B]\int J(r)G(r)dr}$$

$$=\frac{k_B}{2(S+1)}\langle r^2\rangle\ , \tag{18}$$

using the presently determined values of $M(0)\equiv M(0,0)$, $D(0)$, T_C, and the coefficient $D_{5/2}$, and by setting $S=1$. The values so obtained from Eqs. (17) and (18) are compared in Tables I and II.

The observations (i)–(iii) mentioned above assert that the temperature dependence of D cannot be ignored for the amorphous (Fe,Ni)-M alloys studied in this work and the property $D_n \gg D_m$ is inherent to Invar systems (e.g., a-$Fe_{80}B_{20}$ in Table I). This result refutes the earlier claims[32,41] that the wide disparity between the values D_m and D_n of the spin-wave stiffness coefficient usually encountered in Fe-based amorphous (and crystalline) Invar alloys (see the Introduction) completely disappears when contribution to the fractional change in magnetization $\Delta m(T)$ arising from both the spin-wave as well as Stoner single-particle excitations [of either weak itinerant (WI) type[32] or strong itinerant (SI) type[41]] are considered without taking into account the temperature renormalization of D.

IV. DISCUSSION

In order to facilitate a direct comparison between the results of the present investigation and those reported previously on crystalline Fe_xNi_{100-x} alloys, we use the subscript x ($=80p$) instead of p to denote the Fe concentration in the glassy alloys in question in this section. Before proceeding with the discussion, a brief summary of the main findings of this work is given below.

(i) Spin-wave excitations alone seem to account for the observed thermal demagnetization of spontaneous magnetization in a-$Fe_xNi_{80-x}(B,Si)_{20}$ alloys for temperatures below a certain (reduced) temperature t^*, which decreases with increasing x (Fig. 7), but the existence of a small additional contribution from weak-itinerant-type single-particle excitations cannot be ruled out completely. For $t>t^*$, SP excitations of the WI type [Eq. (11b)] are mainly responsible for the decline of magnetization with increasing temperature. As in a-$Fe_xNi_{80-x}(B,Si)_{20}$ alloys for $t<t^*$, the SW contribution completely swamps the WI-type SP contribution in the temperature range $0\lesssim T\lesssim 0.9T_C$ ($0\lesssim T\lesssim 300$ K) for Fe concentrations $x\lesssim 20$ at. % ($30\le x\le 50$) in a-$Fe_xNi_{80-x}P_{14}B_6$ alloys; however, SP excitations of the strong itinerant type [Eq. (11a)] significantly contribute, besides a dominant SW contribution, to thermal demagnetization in the entire temperature range $0\lesssim T\lesssim 300$ K only for $x\gtrsim 60$ at. % in a-$Fe_xNi_{80-x}P_{14}B_6$ alloys. In c-Fe_xNi_{100-x} alloys, a SP

contribution of WI type accompanies a dominant SW contribution throughout the temperature range covered in the experiments (note that SP and SW contributions in these alloys become comparable only for $x \gtrsim 60$ at. %) as is also the case with a-$Fe_xNi_{80-x}(B,Si)_{20}$ and a-$Fe_xNi_{80-x}P_{14}B_6$ alloys in the temperature ranges specified above; the only difference in the crystalline and amorphous alloys is that only in the former case could the SP contribution (coefficient A in Fig. 7) be estimated because of its larger magnitude. (ii) In both the amorphous alloy series, the spin-wave stiffness coefficient D for the alloys with $x \leq 50$ at. % renormalizes with temperature in accordance with the expression [Eq. (16)] predicted by the localized-electron (Heisenberg) model whereas D for Fe concentrations in the range $60 \leq x \leq 80$ follows the temperature variation [Eq. (15)] predicted by the itinerant-electron model. The crossover from $T^{5/2}$ dependence of $D(T)$ to T^2 dependence at $x \simeq 60$ at. % in the presently studied alloy systems constitutes a property which these alloy series share with c-Fe_xNi_{100-x} alloys (Fig. 7); the coefficient $D_{5/2}$ of the $T^{5/2}$ term in Eq. (16) for the amorphous alloys investigated exhibits a dependence on Fe concentration x the same as that observed in c-Fe_xNi_{100-x} alloys and has comparable values in the glass alloys in question and their crystalline counterparts. (iii) While the values of $\langle r^2 \rangle$ for the alloy series I and II (Tables I and II) deduced from Eq. (17) suggest that the range of exchange interactions increases rapidly with x, Eq. (18) predicts that $\langle r^2 \rangle$ decreases with increasing x. (iv) In the concentration range $0 \leq x \leq 60$, the spontaneous magnetization $M(T=0,x)$ versus x curves for a-$Fe_xNi_{80-x}(B,Si)_{20}$ and a-$Fe_xNi_{80-x}P_{14}B_6$ alloys are systematically shifted down with respect to that for c-Fe_xNi_{100-x} alloys by roughly 20 and 40 emu/g, respectively (Fig. 6). However, a sudden drop in $M(T=0,x)$ for $x > 60$ at. % in the c-Fe_xNi_{100-x} series is not observed in the investigated glassy alloys for which $M(T=0,x)$ continues to increase with x but with a progressively slower rate (Fig. 6). (v) The spin-wave stiffness at 0 K, $D(T=0,x)$, and Curie temperature $T_C(x)$ as functions of x go through a broad peak at $x \simeq 60$ at. % ($x \simeq 70$ at. %) for a-$Fe_xNi_{80-x}(B,Si)_{20}$ (a-$Fe_xNi_{80-x}P_{14}B_6$) alloys (Fig. 6). As x is increased beyond 60 at. %, both $D(T=0,x)$ and $T_C(x)$ decrease at a rate which is very steep for the c-Fe_xNi_{100-x} alloys but slows down considerably in the amorphous systems studied; so much so that the decline in these quantities is barely discernible in a-$Fe_xNi_{80-x}P_{14}B_6$ alloys.

Within the framework of the band model, the effect of increasing the Fe concentration x should be to increase the exchange splitting of spin-up ($\uparrow$) and spin-down ($\downarrow$) d subbands (since T_C increases with x, Figs. 1 and 6) and to shift the Fermi level E_F to higher energies [as the spontaneous magnetization $M(0)$ increases with x, Fig. 6]. In this context, the observation (i) above implies that E_F lies within the $d_\uparrow$ and $d_\downarrow$ subbands in the entire composition range for the alloy series I (weak itinerant ferromagnetism), whereas E_F in the alloy series II shifts with x to such an extent that it lies just above the top of the $d_\uparrow$ subband at $x \simeq 60$ at. % where a transition from weak ($x < 60$ at. %) to strong ($x > 60$ at. %) itinerant ferromagnetism takes place. This inference conforms well with the results of spontaneous resistivity anisotropy,[42,43] high-field susceptibility,[43] spin-polarized photoemission,[44] and Compton scattering[45] measurements on the same or similar Fe-Ni amorphous alloys as the present ones. Moreover, the concentration dependence of t^* is consistent with the finding[60] that the temperature range over which the $T^{3/2}$ dependence of spontaneous magnetization in crystalline Fe dominates is confined to temperature $T \lesssim 0.15 T_C$ (or $t^* \simeq 0.15$) only. The theory, due to Lonzarich and Taillefer,[52] based on the itinerant-electron model, yields the following relation between the coefficient A of the T^2 term in Eq. (11b) and the density of single-particle states at E_F, $N(E_F)$:

$$A = \tfrac{1}{2}(2\pi k_B f/\mu)^2 [N(E_F)]^2 \tag{19}$$

with

$$f^2 = \frac{[N'(E_F)/N(E_F)]^2 - [N''(E_F)/N(E_F)]}{3[N'(E_F)/N(E_F)]^2 - [N''(E_F)/N(E_F)]} , \tag{20}$$

where μ is the moment per alloy atom at 0 K in units of μ_B and $N'(E_F)$ [$N''(E_F)$] is the first [second] energy derivative of the density of states (DOS), $N(E)$, at $E = E_F$. Equation (19) permits a calculation of $N(E_F)$ provided the value of the function f [Eq. (20)] is known; the values for the quantities μ and A have already been determined. This requires a complete knowledge about the actual shape of the DOS curve, which is lacking at present for the alloys in question. If we assume that the DOS curve near E_F (around the peak) can be approximated by a Gaussian probability density function, the function f can be expressed as[54]

$$f \simeq 1 - [(\langle E \rangle - E_F)/\sigma]^2 , \tag{21}$$

where the average energy $\langle E \rangle = \int_{-\infty}^{+\infty} E N(E) dE$ and the variance $\sigma^2 = \int_{-\infty}^{+\infty} (E - \langle E \rangle)^2 N(E) dE$. It is evident from Eq. (21) that f attains its maximum value ($=1$) only when $E_F = \langle E \rangle$, i.e., when E_F coincides with the energy at which the DOS curve peaks, and the farther E_F is from $\langle E \rangle$, the lower is the value of f compared to unity. If Eq. (19) with the values for the parameters μ and A determined in this work has to reproduce the $N(E_F)$ values for a-$Fe_xNi_{80-x}B_{20}$ alloys quoted in the literature,[61] f should increase from $\simeq 0.8$ at $x = 20$ at. % to $\simeq 1.0$ at $x = 80$ at. %. In view of Eq. (21), such an increasing trend in f with x should mean that, as x is increased, E_F shifts up but lies below the top of the $d_\uparrow$ DOS curve ($d_\uparrow$ subband) even for $x = 80$ at. % whereas it approaches the peak in the $d_\downarrow$ DOS curve as $x \to 80$ at. %. This deduction supports the above thesis that all the compositions in series I are weak itinerant ferromagnets.

The observation (ii) stated above, far from implying a transition from localized- to itinerant-electron behavior at $x = 60$ at. %, indicates that the magnon-magnon interactions, in the context of the itinerant-electron model [Eq. (14)], weaken with increasing x; so much so that

magnon-SP interactions show up with ease for $x \gtrsim 60$ at. %. It is now well known[26,30,62] that the near-neighbor (NN) configuration of atoms (short-range order) in the Fe-Ni amorphous alloys of present interest is similar to that found in their crystalline counterparts. In view of this result, the finding that $D_{5/2}$ exhibits the same (within the uncertainty limits) variation with x regardless of whether the Fe-Ni alloys are in the crystalline state or in the amorphous state and irrespective of whether the metalloids are present or not suggests that the observed functional dependence of $D_{5/2}$ on x (and hence the reduction in the strength of magnon-magnon interactions with increasing x) is primarily dictated by the alteration in the NN coordination (both type and number) brought about by the change in Fe concentration. Considering that even the slightest change in the NN coordination has a marked influence on the creation or annihilation of short-wavelength magnons, magnon-magnon interactions involving short-wavelength magnons play a decisive role in the temperature renormalization of spin-wave energies. In view of this argument and the finding that the quantities $M(0)$ and $D(0)$ have drastically reduced values in the amorphous state compared to those in the crystalline state (Fig. 6), it is not surprising that the values of $\langle r^2 \rangle$ calculated from Eq. (17) (Tables I and II) underestimate the range of exchange interactions and hence tend to give the misleading impression that such interactions for the glassy alloys with x in the range $0 \lesssim x \lesssim 60$ at. % are confined to the nearest neighbors only. By contrast, the values of $\langle r^2 \rangle$ computed from the $D(0)/T_C$ ratio via Eq. (18) (Tables I and II) provide a better handle on the range of exchange interactions because both $D(0)$ and T_C are directly related to the exchange integral through the expressions given, respectively, by the numerator and denominator in Eq. (18).

Considering that P donates roughly twice as many electrons per atom to the transition metal d bands as B does, the shift in the $M(T=0,x)$ vs x curves [i.e., the observation (iv) above] can be understood[50] in terms of the simple but crude rigid-band model. A steep drop in $M(T=0,x)$, $D(T=0,x)$, and $T_C(x)$ for $x > 60$ at. % in c-Fe_xNi_{100-x} alloys is a manifestation of the Invar effect [i.e., the coexistence of antiferromagnetically coupled (low-spin state) and ferromagnetically coupled (high-spin state) spin pairs]. Alternatively, the antiferromagnetic (AF) interactions build up at the expense of the ferromagnetic interactions in these alloys as x is increased beyond 60 at. % and, as a consequence, a rapid decline in these quantities occurs. In view of these arguments, progressive reduction in the slope $dM(T=0,x)/dx$ and negative values for $dD(T=0,x)/dx$ and $dT_C(x)/dx$ for $x > 60$ at. % in the alloy systems of present interest indicate that the competing (AF plus FM) interactions, more prominent in a-$Fe_{80}B_{20}$ than in a-$Fe_{80}P_{14}B_6$, are present in the alloys with x in the range $60 \lesssim x \leq 80$. This inference is consistent not only with the finding that the ratio D/T_C for a-$Fe_{80}B_{20}$ possesses a value ($=0.14$ meV Å^2/K, Table I) characteristic[34,54] of amorphous ferromagnets with competing interactions, but also with the fact that a-$Fe_{80}B_{20}$ does exhibit[63] Invar behavior. Competing interactions, in turn, give rise to a canted spin arrangement in such ferromagnets. Mössbauer measurements[64] and spin-polarized neutron scattering experiments[65] performed on amorphous Fe-rich (Fe,Ni)-metalloid ($\tilde{M}$) and/or Fe-$\tilde{M}$ alloys do support the existence of noncollinear (canted) spin structure in the alloys with Fe concentration higher than 60 at. %.

At the end of Sec. III, it has already been stated that the present results unambiguously demonstrate that $D_n \gg D_m$ is a characteristic property of the amorphous ferromagnets with competing interactions and/or of amorphous ferromagnetic alloys that exhibit Invar behavior (e.g., a-$Fe_{80}B_{20}$ in Table I). According to Continentino and Rivier,[36] the observed discrepancy between D_m (magnetization) and D_n (inelastic neutron scattering) in such systems can be justified on the following grounds. The diffusive modes, originating from the longitudinal spin fluctuations, make as significant a contribution to the $T^{3/2}$ decrease of magnetization in amorphous canted ferromagnets (i.e., the glassy ferromagnets with a noncollinear ground-state arrangement of spins) as the transverse spin fluctuations (magnons) do, but these diffusions do not give rise to any propagating features in the constant-q INS intensity versus energy scans. Recent triple-axis polarized inelastic neutron scattering data[66] on amorphous $Fe_{86}B_{14}$ (Invar system) and $Fe_{40}Ni_{40}P_{14}B_6$ (non-Invar system) alloys provide strong evidence for the existence of longitudinal spin fluctuations, which, far from being nonpropagating modes (as envisaged by Continentino and Rivier[36]), appear as propagating excitations at energies close to the spin-wave peaks in constant-q scans taken at temperatures well below T_C in both the systems studied. Moreover, these longitudinal propagating excitations, like magnons, follow the dispersion relation $E(T)=D(T)q^2$ and hence give rise to an additional $T^{3/2}$ decrease of magnetization while leaving D_n unaltered from its spin-wave-only value. The possibility of a coupling between transverse (spin-wave) and longitudinal spin fluctuations that leads to propagating longitudinal excitations which peak at spin-wave energies was earlier suggested by several workers.[67–69] Another important observation made by Lynn, Rosov, and Fish[66] is that the intensity of the longitudinal mode peaks is very weak in a-$Fe_{40}Ni_{40}P_{14}B_6$ compared to that in a-$Fe_{86}B_{14}$. This result is in concurrence with our finding (Tables I and II) that the discrepancy between D_m and D_n is more pronounced for a-$Fe_{80}B_{20}$ [$D_n/D_m = 1.85(32)$] than for a-$Fe_{40}Ni_{40}P_{14}B_6$ [$D_n/D_m = 1.13(2)$]. However, none of the theoretical models proposed hitherto[36,67–69] explains why the peaks in the INS spectra belonging to the longitudinal spin fluctuations are more intense in Invar alloys than in non-Invar systems. We attempt an explanation of this finding in terms of the three-dimensional (3D) ferromagnetic matrix plus finite FM spin clusters model,[48,49,54,70] which is applicable to amorphous ferromagnetic alloys only and whose details are given elsewhere.[54,70] According to this model, microscopic regions of low density exist in an otherwise high-density bulk, such that the average nearest-neighbor distance between Fe atoms (and/or Ni atoms that carry negligibly small moment[50] in the

glassy alloys in question) in these "low-density pockets" is appreciably greater than that in the remaining bulk. As a consequence, the ferromagnetic coupling between spins within the finite clusters (low-density regions) is much stronger than that between spins in the FM matrix (high-density bulk). Large quenched-in local stresses exist in the zones that separate these microscopic regions from the bulk, due to considerable mismatch in the NN interatomic spacings within such zones. Wild fluctuations in the NN distance (r_{NN}) within these zones around the critical distance (r_c) at which the exchange integral changes sign in the Bethe-Slater curve give rise to competing interactions which, in turn, result in noncollinear arrangement of spins in the 3D FM matrix in amorphous spin systems. In Invar systems, an additional contribution to the competing interactions arises from strong magnetostrictive coupling between the local quenched-in stresses and spins in the buffer zones surrounding the low-density regions (finite spin clusters). Thus the longitudinal spin fluctuations are more prominent in Invar systems than in non-Invar ones. As the concentration of the moment-bearing (Fe) atoms in the amorphous alloys under consideration increases, the total density decreases (Tables I and II) such that the average NN distance (r_{NN}) between spins in both the FM matrix and the finite spin clusters increases progressively beyond r_c for $x \leq 60$ at. %, whereas for $x > 60$ at. % the low-density regions grow at the expense of the bulk, with the result that r_{NN} between spins in the finite clusters greatly exceeds r_c but r_{NN} is lowered towards r_c for spins in the FM matrix. This process leads to an increase in the average NN (positive) exchange coupling J_{NN} between spins in the FM matrix [and hence in $D(T=0,x)$ and $T_C(x)$] for Fe concentrations up to 60 at. %, but as x is increased beyond 60 at. % J_{NN} decreases and so do $D(T=0,x)$ and $T_C(x)$.

V. SUMMARY AND CONCLUSIONS

The following inferences can be drawn from a detailed analysis and discussion of highly precise magnetization data taken on amorphous $(Fe_pNi_{1-p})_{80}(B,Si)_{20}$ (series I) and $(Fe_pNi_{1-p})_{80}P_{14}B_6$ (series II) alloys.

(i) In series I, the contribution to thermal demagnetization due to single-particle excitations of the weak itinerant type is completely dominated by that arising from spin-wave excitations in the temperature range $0 \lesssim t(=T/T_C) \lesssim t^*(p)$ for all p, but the reverse is true for all the compositions and for temperatures exceeding $t^*(p)$. By contrast, in series II, the SW contribution tends to overshadow a feeble contribution from SP excitations of weak itinerant type in the range of temperatures $3.8\ \text{K} \leq T \leq 0.9T_C (3.8 \leq T \leq 300\ \text{K})$ for Fe concentrations $p \leq 0.25$ $(0.375 \leq p \leq 0.625)$, but for $T \lesssim 300$ K and $p \gtrsim 0.75$ a significant contribution from SP excitations of the strong itinerant type accompanies a dominant SW contribution. This result indicates that all the compositions in the a-$(Fe_pNi_{1-p})_{80}(B,Si)_{20}$ alloy series behave as weak itinerant ferromagnets while a transition from weak itinerant to strong itinerant ferromagnetism occurs at a concentration $p \simeq 0.75$ in the a-$(Fe_pNi_{1-p})_{80}P_{14}B_6$ alloy series.

(ii) In both the alloy series, the spin-wave stiffness coefficient D varies with temperature as $T^{5/2}$ for Fe concentrations up to $p \simeq 0.625$ whereas $D(T)$ is best described by the T^2 power law in the concentration range $0.75 \leq p \leq 1.0$. The crossover from $T^{5/2}$ dependence of $D(T)$ to T^2 dependence at $p \simeq 0.75$ (or $x \simeq 60$ at. %) constitutes a property which the glassy alloys in question share with the fcc Fe_xNi_{100-x} crystalline alloys. Within the framework of the itinerant-electron model, this observation implies that the magnon-magnon interactions (especially the ones that involve short-wavelength magnons) weaken with increasing p; so much so that magnon-SP interactions show up with ease for $p \gtrsim 0.75$.

(iii) The present results unambiguously demonstrate that D_n (the value of D determined from either inelastic neutron scattering or Brillouin scattering experiments) $\gg D_m$ (the value of D deduced from the magnetization measurements) is a characteristic property of the amorphous ferromagnets with competing interactions and/or of amorphous ferromagnetic alloys that exhibit Invar behavior. Based on the observed Fe concentration dependence of $M(T=0,p)$, $D(T=0,p)$, and $T_C(p)$ in the investigated amorphous alloys, it is argued that the competing interactions present in the alloys with p in the range $0.75 \lesssim p \lesssim 1.0$ give rise to a noncollinear (canted) arrangement of spins in the ground state. The property $D_n \gg D_m$ of the amorphous alloys with $p > 0.75$ is a consequence of the fact that, owing to the canted spin structure, longitudinal spin fluctuations make as significant a contribution to the $T^{3/2}$ decrease of magnetization as the transverse spin fluctuations (spin waves) do but leave D_n unaltered from its spin-wave-only value.

(iv) The direct exchange interactions extend beyond the second nearest-neighbor distance for compositions close to, but above, the critical concentration for the appearance of long-range ferromagnetic order, whereas the competing interactions in the amorphous alloys with $p > 0.75$ confine them (direct d-d exchange interactions) to the nearest neighbors only.

(v) The composition dependence of D and T_C observed in this work as well as the recent finding that the peaks in the INS spectra due to the longitudinal spin fluctuations are more intense in Invar alloys than in non-Invar systems find a straightforward explanation in terms of the model of three-dimensional (infinite) ferromagnetic matrix plus finite FM spin clusters.

ACKNOWLEDGMENTS

Part of the work presented here was carried out at the Ruhr Universität Bochum, Germany, by one of the authors (S.N.K.) who thanks Professor S. Methfessel for providing the required experimental facilities. The financial support from the Department of Atomic Energy, India, under Project No. 37/10/93-G/6 is also gratefully acknowledged.

*Author to whom all the correspondence should be addressed.

[1]J. D. Axe, L. Passell, and C. C. Tsuei, in *Magnetism and Magnetic Materials—1974 (San Francisco),* Proceedings of the 20th Annual Conference on Magnetism and Magnetic Materials, edited by C. D. Graham, Jr., G. H. Lander, and J. J. Rhyne, AIP Conf. Proc. No. 24 (AIP, New York, 1975), p. 119; H. A. Mook, N. Wakabayashi, and D. Pan, Phys. Rev. Lett. **34**, 1029 (1975).

[2]J. W. Lynn, G. Shirane, R. J. Birgeneau, and H. S. Chen, in *Magnetism and Magnetic Materials—1976 (Joint MMM-Intermag Conference, Pittsburgh),* Proceedings of the First Joint MMM-Intermag Conference, edited by J. J. Becker and G. H. Lander, AIP Conf. Proc. No. 34 (AIP, New York, 1976), p. 313.

[3]J. D. Axe, G. Shirane, T. Mizoguchi, and K. Yamauchi, Phys. Rev. B **15**, 2763 (1977); H. A. Mook and C. C. Tsuei, *ibid.* **16**, 2184 (1977).

[4]J. A. Tarvin, G. Shirane, R. J. Birgeneau, and H. S. Chen, Phys. Rev. B **17**, 241 (1978); R. J. Birgeneau, J. A. Tarvin, G. Shirane, E. M. Gyorgy, R. C. Sherwood, and H. S. Chen, *ibid.* **18**, 2192 (1978).

[5]H. Grimsditch, A. Malozemoff, and A. Brunsch, Phys. Rev. Lett. **43**, 711 (1979).

[6]Y. Ishikawa, K. Yamada, K. Tajima, and K. Fukamichi, J. Phys. Soc. Jpn. **50**, 1958 (1981).

[7]J. J. Rhyne, G. E. Fish, and J. W. Lynn, J. Appl. Phys. **53**, 2316 (1982).

[8]Z. Xianyu, Y. Ishikawa, and S. Onodera, J. Phys. Soc. Jpn. **51**, 1799 (1982).

[9]H. A. Mook and J. W. Lynn, Phys. Rev. B **29**, 4056 (1984).

[10]W. Minor, B. Lebech, K. Clausen, and W. Dmowski, in *Rapidly Quenched Metals,* edited by S. Steeb and H. Warlimont (Elsevier, Amsterdam, 1985), p. 1149.

[11]J. A. Fernandez-Baca, J. J. Rhyne, and G. E. Fish, J. Magn. Magn. Mater. **54-57**, 289 (1986); J. A. Fernandez-Baca, J. W. Lynn, J. J. Rhyne, and G. E. Fish, J. Appl. Phys. **61**, 3406 (1987).

[12]J. A. Fernandez-Baca, J. W. Lynn, J. J. Rhyne, and G. E. Fish, Phys. Rev. B **36**, 8497 (1987).

[13]J. W. Lynn and J. J. Rhyne, in *Spin Waves and Magnetic Excitations,* edited by A. S. Borovik-Romanov and S. K. Sinha (Elsevier, Amsterdam, 1988), Part II, Chap. 4, p. 177.

[14]J. A. Fernandez-Baca, J. J. Rhyne, G. E. Fish, M. Hennion, and B. Hennion, J. Appl. Phys. **67**, 5223 (1990); S. C. Yu, J. W. Lynn, and G. E. Fish, Jpn. J. Appl. Phys. **32**, 67 (1993).

[15]F. Keffer, in *Encyclopedia of Physics,* edited by H. P. J. Wijn (Springer, Berlin, 1966), Vol. XVIII, Part 2, p. 1.

[16]R. W. Cochrane and G. S. Cargill III, Phys. Rev. Lett. **32**, 476 (1974).

[17]C. C. Tsuei and H. Lilienthal, Phys. Rev. B **13**, 4899 (1976).

[18]T. Mizoguchi, in *Magnetism and Magnetic Materials-1976* (Ref. 2), p. 286.

[19]C. L. Chien and R. Hasegawa, Phys. Rev. B **16**, 2115 (1977); **16**, 3024 (1977).

[20]N. S. Kazama, M. Mitera, and T. Masumoto, in *Proceedings of the Third International Conference on Rapidly Quenched Metals, Brighton, 1978,* edited by B. Cantor (The Metals Socieity, London, 1978), p. 164.

[21]S. M. Bhagat, M. L. Spano, and K. V. Rao, J. Appl. Phys. **50**, 1580 (1979); S. Hatta and T. Egami, *ibid.* **50**, 1589 (1979).

[22]R. Hasegawa and R. Ray, Phys. Rev. B **20**, 211 (1979).

[23]C. L. Chien, D. Musser, E. M. Gyorgy, R. C. Sherwood, H. S. Chen, F. E. Luborsky, and J. L. Walter, Phys. Rev. B **20**, 283 (1979).

[24]S. Dey, U. Gorres, H. J. V. Nielsen, M. Rosenberg, and M. Sostarich, J. Phys. (Paris) Colloq. **41**, C8-678 (1980); S. Dey, P. Deppe, M. Rosenberg, F. E. Luborsky, and J. L. Walter, J. Appl. Phys. **52**, 1805 (1981).

[25]G. Hilscher, R. Haferl, H. Kirchmayr, M. Müller, and H. J. Güntherodt, J. Phys. F **11**, 2429 (1981).

[26]S. N. Kaul, Phys. Rev. B **24**, 6550 (1981).

[27]M. Sostarich, S. Dey, P. Deppe, M. Rosenberg, G. Czjzek, V. Oestreich, H. Schmidt, and F. E. Luborsky, IEEE Trans. Magn. **MAG-17**, 2612 (1981).

[28]G. Bayreuther, G. Enders, H. Hoffmann, U. Korndörfer, W. Oestreicher, K. Röll, and M. Takahashi, J. Magn. Magn. Mater. **31-34**, 1535 (1983).

[29]A. K. Majumdar, V. Oestreich, D. Weschenfelder, and F. E. Luborsky, Phys. Rev. B **27**, 5618 (1983).

[30]S. N. Kaul, Phys. Rev. B **27**, 5761 (1983); **27**, 6923 (1983).

[31]K. Hüller and G. Dietz, J. Magn. Magn. Mater. **50**, 250 (1985); K. Hüller, *ibid.* **61**, 347 (1986).

[32]O. Yamada, M. Mimura, H. Maruyama, I. Nakai, S. Ishio, and M. Takahashi, J. Magn. Magn. Mater **54-57**, 250 (1986).

[33]I. Nakai, O. Yamada, M. Mimura, S. Ishio, and M. Takahashi, J. Phys. Soc. Jpn. **56**, 4056 (1987).

[34]S. N. Kaul and T. V. S. M. Mohan Babu, J. Phys. Condens. Matter **1**, 8509 (1989).

[35]Z. Xianyu, Y. Ishikawa, S. Ishio, and M. Takahashi, J. Phys. F **15**, 1787 (1985).

[36]M. A. Continentino and N. Rivier, J. Phys. F **9**, L145 (1979); N. Rivier and M. A. Continentino, J. Magn. Magn. Mater. **15-18**, 1419 (1980).

[37]H. Mano, J. Phys. Soc. Jpn. **51**, 3157 (1982).

[38]E. P. Wohlfarth, J. Magn. Magn. Mater. **10**, 120 (1979).

[39]S. N. Kaul and M. Rosenberg, Phys. Rev. B **25**, 5863 (1982).

[40]S. N. Kaul, Solid State Commun. **52**, 1015 (1984); T. Egami, Rep. Prog. Phys. **47**, 1601 (1984).

[41]E. Babic, Z. Marohnic, and E. P. Wohlfarth, Phys. Lett. **95A**, 335 (1983).

[42]S. N. Kaul, Phys. Status Solidi B **116**, K99 (1983).

[43]S. N. Kaul and M. Rosenberg, Phys. Rev. B **27**, 5698 (1983).

[44]H. Hopster, R. Kurzawa, R. Raue, W. Schmidt, G. Gütherodt, K. H. Walker, and H. J. Güntherodt, J. Phys. F **15**, L11 (1985).

[45]A. Anderjczuk, L. Dobrzynski, E. Zukowski, M. J. Cooper, S. Hamouda, and J. Latuszkiewiz, J. Phys. Condens. Matter **4**, 2735 (1992).

[46]S. N. Kaul, Phys. Rev. B **38**, 9178 (1988).

[47]S. N. Kaul and M. Sambasiva Rao, Phys. Rev. B **43**, 11 240 (1991), and J. Phys. Condens. Matter (to be published).

[48]S. N. Kaul, J. Magn. Magn. Mater. **53**, 5 (1985); IEEE Trans. Magn. **MAG-20**, 1290 (1984).

[49]S. N. Kaul, Solid State Commun. **36**, 279 (1980).

[50]S. N. Kaul, IEEE Trans. Magn. **MAG-17**, 1208 (1981).

[51]J. Mathon and E. P. Wohlfarth, Proc. R. Soc. London Ser. A **302**, 409 (1968).

[52]G. Lonzarich and L. Taillefer, J. Phys. C **18**, 4339 (1985).

[53]J. Takeuchi and Y. Masuda, J. Phys. Soc. Jpn. **46**, 468 (1979).

[54]S. N. Kaul, J. Phys. Condens. Matter **3**, 4027 (1991), and the references cited therein; S. N. Kaul and P. D. Babu, *ibid.* **4**, 6429 (1992).

[55]T. Izuyama and R. Kubo, J. Appl. Phys. **35**, 1074 (1964).

[56]S. M. Bhagat, D. J. Webb, and M. A. Manheimer, J. Magn. Magn. Mater. **53**, 209 (1985); D. J. Webb and S. M. Bhagat, *ibid.* **42**, 109 (1984).

[57]Z. Frait and D. Fraitova, Phys. Status Solidi B **154**, 363 (1989); Z. Frait and D. Fraitova, in *Spin Waves and Magnetic Excitations* (Ref. 13), Vol. 2, p. 1.
[58]I. Nakai, J. Phys. Soc. Jpn. **52**, 1781 (1983); I. Nakai, F. Ono, and O. Yamada, *ibid.* **52**, 1791 (1983).
[59]J. Crangle and G. C. Hallam, Proc. R. Soc. London Ser. A **272**, 119 (1963).
[60]B. E. Argyle, S. H. Charap, and E. W. Pugh, Phys. Rev. **132**, 2051 (1963).
[61]D. G. Onn, A. Sundermier, and J. K. Krause, J. Appl. Phys. **52**, 1802 (1981).
[62]V. Dose, in *Rapidly Quenched Metals* (Ref. 10), p. 963.
[63]F. Fukamichi, T. Masumoto, and M. Kikuchi, IEEE Trans. Magn. **MAG-15**, 1404 (1979).
[64]S. J. Harker and R. J. Pollard, J. Phys. Condens. Matter **1**, 8269 (1989).
[65]R. A. Cowley, C. Patterson, N. Cowlam, P. K. Ivison, J. Martinez, and L. D. Cussen, J. Phys. Condens. Matter **3**, 9521 (1991).
[66]J. W. Lynn, N. Rosov, and G. E. Fish, J. Appl. Phys. **73**, 5369 (1993).
[67]V. G. Vaks, A. I. Larkin, and S. A. Pikin, Zh. Eksp. Teor. Fiz. **53**, 1089 (1967) [Sov. Phys. JETP **26**, 647 (1968)].
[68]R. Raghavan and D. L. Huber, Phys. Rev. B **14**, 1185 (1976).
[69]J. K. Bhattacharjee, Phys. Rev. B **27**, 3058 (1983).
[70]S. N. Kaul, V. Siruguri, and G. Chandra, Phys. Rev. B **45**, 12 343 (1992).